⌘ *Author's Choice*

Myosin and Tropomyosin Stabilize the Conformation of Formin-nucleated Actin Filaments*⒮

Zoltán Ujfalusi[‡§¶], **Mihály Kovács**[‖1], **Nikolett T. Nagy**[‖], **Szilvia Barkó**[‡§], **Gábor Hild**[‡§], **András Lukács**[‡§], **Miklós Nyitrai**[‡§2], **and Beáta Bugyi**[‡§3]

From the ‡Department of Biophysics, Medical School, University of Pécs, Szigeti Street 12, H-7624 Pécs, Hungary, §Szentágothai Research Center, Ifjúság Street 34, H-7624 Pécs, Hungary, ¶Office for Subsidized Research Units, Hungarian Academy of Sciences, Nádor Street 7, H-1051 Budapest, Hungary, and ‖Eötvös Loránd University-Hungarian Academy of Sciences "Momentum" Motor Enzymology Research Group, Department of Biochemistry, Faculty of Science, Eötvös Loránd University, Pázmány Péter Esplanade 1/c, H-1117 Budapest, Hungary

Background: The regulation of the conformational dynamics of cellular actin structures is poorly understood.
Results: Myosin and tropomyosin stabilize the conformation of formin-nucleated flexible actin filaments.
Conclusion: Actin-binding proteins can play a central role in the establishment of the conformational properties of actin filaments.
Significance: Our results add to our understanding of the mechanisms regulating the conformational and functional versatility of the actin cytoskeleton.

The conformational elasticity of the actin cytoskeleton is essential for its versatile biological functions. Increasing evidence supports that the interplay between the structural and functional properties of actin filaments is finely regulated by actin-binding proteins; however, the underlying mechanisms and biological consequences are not completely understood. Previous studies showed that the binding of formins to the barbed end induces conformational transitions in actin filaments by making them more flexible through long range allosteric interactions. These conformational changes are accompanied by altered functional properties of the filaments. To get insight into the conformational regulation of formin-nucleated actin structures, in the present work we investigated in detail how binding partners of formin-generated actin structures, myosin and tropomyosin, affect the conformation of the formin-nucleated actin filaments using fluorescence spectroscopic approaches. Time-dependent fluorescence anisotropy and temperature-dependent Förster-type resonance energy transfer measurements revealed that heavy meromyosin, similarly to tropomyosin, restores the formin-induced effects and stabilizes the conformation of actin filaments. The stabilizing effect of heavy meromyosin is cooperative. The kinetic analysis revealed that despite the qualitatively similar effects of heavy meromyosin and tropomyosin on the conformational dynamics of actin filaments the mechanisms of the conformational transition are different for the two proteins. Heavy meromyosin stabilizes the formin-nucleated actin filaments in an apparently single step reaction upon binding, whereas the stabilization by tropomyosin occurs after complex formation. These observations support the idea that actin-binding proteins are key elements of the molecular mechanisms that regulate the conformational and functional diversity of actin filaments in living cells.

In the eukaryotic cytoskeleton, dynamic actin networks are essential for many biological processes, such as the establishment of cell shape, cell migration, cell division, and intracellular transport (1–3). These functions require certain mechanical stability and conformational properties of actin filaments (F-actin). Probably in correlation with the many complex intracellular functions of actin, the conformation of actin filaments proved to be sensitive to changes in various environmental parameters (4–7) and also to the binding of peptides (8) and actin-binding proteins (9–14). However, in many cases, the mechanisms regulating the coupling between conformational and functional polymorphism of actin structures are not completely understood.

Assembly factors are central to achieve rapid, spatiotemporally controlled formation of cellular actin networks (15–17). Among these factors, formin proteins catalyze the nucleation and processive growth of linear actin filaments that compose actin structures, such as the cytokinetic ring, stress fibers, and actin cables (18). Recent studies by us and other groups revealed that formins alter the conformational state of actin

[1] Bolyai Fellow of the Hungarian Academy of Sciences.
[2] Holds a Wellcome Trust International Senior Research Fellowship in Biomedical Sciences.
[3] Bolyai Fellow of the Hungarian Academy of Sciences. To whom correspondence should be addressed: University of Pécs, Medical School, Dept. of Biophysics, Pécs, Szigeti str. 12, H-7624 Hungary. Tel.: 36-72-536-265; Fax: 36-72-536-261; E-mail: beata.bugyi@aok.pte.hu.

filaments (19 –23). The binding of a single formin homology 2 (FH2)[4] dimer from mammalian Diaphanous-related protein 1 from mouse (mDia1) formin (mDia1-FH2) to the barbed end induces a more flexible conformation of actin filaments through long range allosteric effects (20 –22). Bnr1 but not Bni1 from the yeast *Saccharomyces cerevisiae* was also proposed to cause a significant change in filament conformation (19). Importantly, formin-induced structural changes are accompanied by altered functional properties of actin filaments (20).

Formin-generated actin structures interact with many actin-binding proteins, which can influence the formin-induced conformational transitions. One of these interacting proteins, tropomyosin (TM), was shown to reverse the formin-induced conformational changes and stabilize the structure of the filaments (24). Myosin is one of the most abundant actin-binding proteins that also localizes to formin-nucleated actin structures in cells (25, 26). Myosin binding to actin filaments induces long range allosteric and cooperative effects in the conformation of the filaments (27–30), which were shown to be dependent on the myosin isoform (31). Thus, myosin can be another candidate for the regulation of the conformational dynamics of formin-nucleated actin structures.

In the present work, we investigated in detail how double-headed heavy meromyosin (HMM) and skeletal tropomyosin influence the conformation of formin-nucleated actin filaments using steady-state fluorescence anisotropy, fluorescence anisotropy decay, and temperature-dependent Förster-type resonance energy transfer (FRET) measurements. We identified HMM as another binding partner of the formin-nucleated actin structures that stabilizes the formin-generated flexible actin filaments upon binding. The results indicate that stabilizing effects of HMM and TM are qualitatively similar but kinetically markedly different. Our findings support the idea that certain actin-binding proteins play a regulatory role in the fine tuning of the structural properties of actin.

EXPERIMENTAL PROCEDURES

Materials—CaCl₂, KCl, MgCl₂, Tris-HCl, glycogen, *N*-(-iodo-acetaminoethyl)-1-naphtylamine-5-sulfonic acid (IAEDANS), 5-(iodoacetamido)fluorescein (IAF), EGTA, phenylmethanesulfonyl fluoride (PMSF), DTT, NaN₃, α-chymotrypsin, ammonium sulfate, thrombin, ATP, and β-mercaptoethanol were obtained from Sigma. Dimethyl sulfoxide (DMSO) was obtained from Fluka (Buchs, Switzerland).

Protein Preparation and Purification—Powder of acetone-dried rabbit skeletal muscle was made as described previously (32). Rabbit skeletal muscle actin was prepared according to the method of Spudich and Watt (33) and stored in a buffer containing 4 mM Tris-HCl (pH 7.3), 0.2 mM ATP, 0.1 mM CaCl₂, and 0.5 mM DTT (buffer A). The concentration of G-actin was determined spectrophotometrically using the absorption coefficient 0.63 ml mg^{-1} cm^{-1} at 290 nm (34) and the relative molecular mass of 42,300 Da for G-actin (35).

The FH2 fragment of mDia1 formin was expressed as a glutathione transferase fusion protein in *Escherichia coli* BL21 (DE3)pLysS strain (36). Protein expression was induced with isopropyl β-D-thiogalactopyranoside. The cell lysate was clarified and loaded onto a GSH column (Amersham Biosciences). The glutathione transferase fusion formin was cleaved with thrombin and eluted from the column. Further purification was done with size exclusion chromatography (Sephacryl S-300). The concentration of mDia1-FH2 was determined spectrophotometrically using the absorption coefficient $\epsilon_{280} = 21.680$ M^{-1} cm^{-1} at 280 nm (ProtParam). The formin concentrations given in this study are mDia1-FH2 monomer concentrations.

HMM was prepared with the method described by Margossian and Lowey (37). The concentration of HMM was determined spectrophotometrically using the absorption coefficient 0.56 ml mg^{-1} cm^{-1} at 280 nm. The HMM concentrations given in this study are HMM monomer (head) concentrations.

Skeletal muscle tropomyosin was prepared from rabbit skeletal muscle according to Smillie (38). The concentration of TM was determined spectrophotometrically using the absorption coefficient 0.3 ml mg^{-1} cm^{-1} at 280 nm. The purified proteins were frozen in liquid nitrogen and stored at −80 °C.

Fluorescent Labeling of Actin—Actin monomers were labeled fluorescently with either IAEDANS or IAF dye at Cys^{374} (see Fig. 1, *left panel*). The labeling with IAEDANS was carried out according to the method of Miki *et al.* (39). 2 mg/ml F-actin (in DTT-free buffer A supplemented with 100 mM KCl and 2 mM MgCl₂) was incubated with a 10-fold molar excess of IAEDANS at room temperature for 1 h. The label was first dissolved in ~50 μl of DMSO, and then DTT-free buffer A was added to the solution (drop by drop until 800 μl) before being added to the protein. The final concentration of DMSO was always lower than 0.5% (v/v) in the samples. After incubation, the labeling was terminated with 2 mM β-mercaptoethanol. The sample was ultracentrifuged (100,000 × *g* for 30 min at 4 °C). The pellet was gently homogenized with a Teflon homogenizer and dialyzed overnight against buffer A at 4 °C. The concentration of the fluorescent dye in the protein solution was determined using the absorption coefficient 6100 M^{-1} cm^{-1} at 336 nm for actin-bound IAEDANS (40). The molar ratio of the bound probe to actin monomers was determined to be 0.8 – 0.9.

Labeling Cys^{374} of actin with IAF (see Fig. 1, *left panel*) was performed according to standard procedures (5). G-actin (2 mg/ml) was labeled in DTT-free buffer A with a 15-fold molar excess of IAF. IAF was dissolved in 0.1 N NaOH and added to the actin solution drop by drop at room temperature while the pH was kept constant. The sample was incubated at 4 °C for 24 h. After incubation, the actin was polymerized for 2 h at room temperature by the addition of 2 mM MgCl₂ and 100 mM KCl and ultracentrifuged (100,000 × *g* for 30 min at 4 °C). The pellet was treated in a way similar to that described for IAEDANS labeling. The concentration of the probe was determined using the absorption coefficient 60,000 M^{-1} cm^{-1} at 495 nm. The molar ratio of the bound probe to actin monomers was 0.6 – 0.7.

Preparation of the Samples—Samples were freshly prepared both for steady-state and time-dependent fluorescence measurements. The actin-bound calcium was replaced with mag-

---

[4] The abbreviations used are: FH2, formin homology 2; mDia1, mammalian Diaphanous-related protein 1 from mouse; TM, tropomyosin; HMM, heavy meromyosin; IAEDANS, *N*-(-iodoacetaminoethyl)-1-naphtylamine-5-sulfonic acid; IAF, 5-(iodoacetamido)fluorescein; S1, myosin subfragment-1; *f*′, normalized FRET efficiency; Δ*r*, anisotropy increase.

nesium by adding 0.2 mM EGTA and 0.05 mM MgCl$_2$ (final concentrations) and incubating the samples for 5–10 min. To initiate the polymerization, the final concentration of MgCl$_2$ and KCl was adjusted to 1 and 50 mM, respectively. In time-dependent anisotropy and temperature-dependent FRET measurements, mDia1-FH2 and HMM were added to actin at the beginning of the polymerization, and then the samples were incubated overnight at 4 °C. In steady-state anisotropy measurements, HMM and TM were added to preformed actin filaments incubated overnight at 4 °C.

The total sample volume was 1 ml in anisotropy decay and steady-state anisotropy experiments and 100 μl in temperature-dependent FRET measurements. Before the measurements, the samples were incubated at room temperature for at least 30 min.

Steady-state Fluorescence Experiments—Steady-state fluorescence measurements were carried out with a Horiba Jobin Yvon Fluorolog-3 luminescence spectrometer equipped with a thermostated sample holder (HAAKE F3 heating bath and circulator (HAAKE Mess-Technik GmbH Co., Karlsruhe, Germany)).

Temperature-dependent FRET Measurements—On the basis of the theory developed by Somogyi *et al.* (41, 42), FRET can be used to probe the changes in the internal conformational transitions within proteins. The rate constant of FRET is inversely proportional to the 6th power of the relative distance between the donor and the acceptor molecules. This parameter is sensitive to the changes in the relative fluctuations and conformational transitions of the protein matrix. A straightforward way to affect intramolecular motions is to change the temperature. The temperature profile of the rate constant of FRET can reflect the relative changes in the conformational dynamics of proteins. However, in practice, it is difficult to directly measure the rate constant of FRET. To overcome this problem, a special FRET parameter proportional to the rate constant of FRET, the normalized FRET efficiency (f'), was introduced.

$$f' = \frac{E}{F_{DA}} \qquad \text{(Eq. 1)}$$

where E is the FRET efficiency and F_{DA} is the fluorescence emission of the donor in the presence of the acceptor. E can be calculated as follows.

$$E = 1 - \frac{F_{DA}}{F_D} \qquad \text{(Eq. 2)}$$

where F_D is the fluorescence emission of the donor in the absence of the acceptor.

The temperature dependence of f' can give information about the conformational state of the investigated protein (41, 42): the steeper the temperature dependence of f', the more dynamic the protein conformation. In practice, the relative f' is calculated as the ratio of the value of f' at the given temperature and the value of f' at the lowest temperature (6 °C). This parameter is independent from the quantum yield of the fluorophore. This parameter can reflect the relative but not the absolute changes in the conformational dynamics of actin filaments. In the analysis, the rela-

tive f' obtained at the highest temperature (34 °C) was plotted as the function of HMM concentration.

In FRET measurements, IAEDANS and IAF served as donor and acceptor, respectively. The donor and the acceptor were attached to different actin protomers within the filament. This experimental strategy allows investigation of the intermonomer conformational dynamics of actin filaments. To measure F_D, donor-containing samples were prepared by mixing IAEDANS-labeled and unlabeled actin monomers in a 1:9 ratio. To measure F_{DA}, donor-acceptor-containing samples were prepared by mixing actin monomers labeled with either IAEDANS or IAF. The ratio of the IAEDANS-labeled monomers to the IAF-labeled monomers was 1:9. This relatively low donor ratio ensures that there is no acceptor in the filament that is in energy transfer with more than one donor molecule.

The fluorescence intensity of IAEDANS was recorded in the absence and presence of IAF at different temperatures between 6 and 34 °C. The excitation wavelength for IAEDANS was 350 nm. The optical slit was set to 1 and 10 nm in the excitation and emission sides, respectively. To obtain F_D and F_{DA}, the measured fluorescence intensities were corrected for the inner filter effect and integrated over the wavelength range of 440–460 nm. The FRET experiments were carried out with 5 μM actin, 500 nM mDia1-FH2, and HMM as indicated.

Steady-state Anisotropy Measurements—In steady-state anisotropy measurements, the time dependence of the anisotropy of IAEDANS-labeled actin was monitored in the absence or presence of the investigated actin-binding proteins. Measurements were carried out using 5 μM actin and 500 nM mDia1-FH2. When applicable, HMM or TM at the indicated concentrations was added to formin-nucleated actin filaments after full polymerization.

The sample was excited with plane-polarized light at 350 nm, and the degree of polarization of the emitted fluorescence was detected at 470 nm. The kinetics of the change in the steady-state anisotropy ($r_{ss}(t)$) was analyzed by fitting an exponential function to the experimental data using the following equation.

$$r_{ss}(t) = r_{max} - \Delta r \times \exp(-k_{obs} \times t) \qquad \text{(Eq. 3)}$$

where r_{max} is the final (maximum) anisotropy, Δr is the difference between the initial and final anisotropy (*anisotropy increase*), t is the time, and k_{obs} is the rate constant of the anisotropy increase. For further analysis, Δr or k_{obs} was plotted as a function of the HMM or TM concentration and fitted by a hyperbolic function using the following equation.

$$y = \text{Max} \frac{c}{K_{1/2} + c} \qquad \text{(Eq. 4)}$$

where Max is the maximum increase of Δr or k_{obs} obtained at a saturating amount of HMM or TM, $K_{1/2}$ is the half-saturating concentration, and c is the concentration of HMM or TM.

Time-dependent Fluorescence Anisotropy Experiments—Time-dependent fluorescence measurements were carried out with an ISS K2 multifrequency phase fluorometer (ISS Fluorescence Instrumentation, Champaign, IL) using the frequency cross-correlation method. The temperature was maintained with a HAAKE F3 heating bath and circulator (HAAKE Mess-Tech-

nik GmbH Co.). The excitation light was provided by a 300-watt xenon arc lamp and modulated with a double crystal Pockels cell. The samples were excited at 350 nm, and emission was monitored through a 385FG03-25 high pass filter. Modulation frequency was changed in 10 steps (evenly distributed on a logarithmic scale) from 5 to 80 MHz in fluorescence lifetime measurements and in 15 steps from 2 to 100 MHz in anisotropy decay measurements (representative data are shown in Fig. 2A). The phase delay and demodulation of the sinusoidally modulated fluorescence signal were measured with respect to the phase delay and demodulation of a standard reference substance. Freshly prepared glycogen solution was used as a lifetime reference. As this solution did not contain fluorophore, the scattered light had an apparent fluorescence lifetime of 0 ns. The data were analyzed by Vinci 1.6 decay analysis software. The goodness of fit was determined from the value of the reduced χ^2 defined as in Lakowicz (43). In the analyses, we assumed constant, frequency-independent error in both phase angle ($\pm 0.200°$) and modulation ratio (± 0.004).

In fluorescence lifetime measurements, the best fits were obtained when we applied double exponential decay for the analyses. The anisotropy data were fitted to the following double exponential function (43).

$$r(t) = r_1 \exp(-t/\varphi_1) + r_2 \exp(-t/\varphi_2)$$ (Eq. 5)

where φ_1 and φ_2 are rotational correlation times with amplitudes r_1 and r_2.

To describe the conformational dynamics of the microenvironment of IAEDANS attached to Cys[374], the two-dimensional angular range of the cone (half-angle, Θ) within which the fluorophore performs wobbling motion was estimated from the amplitudes of the two rotational modes resolved in anisotropy decay measurements according to the following equation (44).

$$\frac{r_2}{r_1 + r_2} = \frac{\cos^2\Theta(1 + \cos\Theta)^2}{4}$$ (Eq. 6)

where r_1 and r_2 are the amplitudes of the faster and slower exponential decay components, respectively. In the fluorescence anisotropy decay measurements, the concentration of actin and mDia1-FH2 were 30 and 1.25 μM, respectively, and the concentration of HMM was as indicated.

Analysis of the Cooperativity—Actin-binding proteins often exert their effects on the conformation of actin filaments cooperatively. Cooperativity in this case means that the binding of a partner molecule can change the conformation of actin protomers distant from the binding site. One way of describing this cooperative effect is to define a cooperative unit, *i.e.* the set of actin protomers that are affected by the binding of one partner molecule. In this work, we estimated the length of the cooperative unit (N) using the linear lattice model and the following equation (28).

$$p = p_1 - (p_1 - p_2)(1 - \alpha)^N$$ (Eq. 7)

where p is either the longer rotational correlation time from anisotropy decay experiments or the value of the relative f' at the highest temperature; p_1 and p_2 denote the limiting values of the corresponding parameters obtained in the absence of

HMM and at saturating HMM concentrations, respectively; and α is the binding density of HMM to actin. Note that this equation allowed the fitting below $\alpha = 1$. As in strong binding states, the binding of HMM to actin is tight, so we take the value of α as the HMM head:actin monomer concentration ratio. Because of this approximation, the N values obtained from these fits somewhat underestimate the lengths of the cooperative units.

RESULTS

HMM Stabilizes the Formin-nucleated Actin Filaments— Previous studies proved that the binding of formins to the barbed end increases the flexibility of actin filaments, resulting from more tenuous interactions between actin protomers in formin-nucleated actin filaments (20–22). This formin-induced conformational transition was reversed by the binding of TM to actin filaments (24). In the present work, we investigated the effects of myosin, another common binding partner of the formin-generated actin structures, on the conformation of the formin-nucleated actin filaments.

As full-length myosin precipitates at relatively low ionic strengths, *i.e.* under the experimental conditions applied here, we used myosin fragments for the investigations. First, we measured the effect of the single-headed myosin subfragment-1 (S1) in nucleotide-free solutions in which the actin binding affinity of S1 is high enough to achieve a high degree of saturation even at moderate S1 concentrations. In the absence of nucleotide, we could not detect the previously observed effect of mDia1-FH2 on the conformational dynamics of actin filaments (data not shown). This observation supports the previous findings as nucleotides play an important role in the interaction of formin with actin (45, 46). Therefore, the use of nucleotides was necessary to assess the effect of myosin on the structure of formin-nucleated actin filaments. For this reason, we used double-headed HMM, which has substantially higher affinity for actin than S1 due to the simultaneous binding of two heads to adjacent sites of the actin filament (47). In this way, we could achieve a high degree of saturation of the myosin binding sites on actin even in the presence of nucleotides without using very high protein concentrations.

First, we assessed the effect of HMM on the conformational dynamics of formin-nucleated actin filaments in time-dependent anisotropy decay experiments. This approach proved to be very powerful in our previous work to describe the conformational properties of actin under various conditions (5, 48, 49). The measurements were carried out with IAEDANS-actin filaments labeled at Cys[374] (Fig. 1, *left panel*). The analysis of the data (Fig. 2A) resolved two rotational correlation times. On the basis of our previous studies, the shorter rotational correlation time can be related to the motion of the probe relative to the protein, which does not show significant changes when the conformational state of the actin filament is altered. In contrast, the longer rotational correlation time can reflect the changes in the conformation of actin filaments upon interaction with binding partners (50). Consistently, in the present study, the value of the shorter rotational correlation time showed no formin or HMM concentration dependence, and its value was between 1 and 3 ns (data not shown). In the absence of actin-
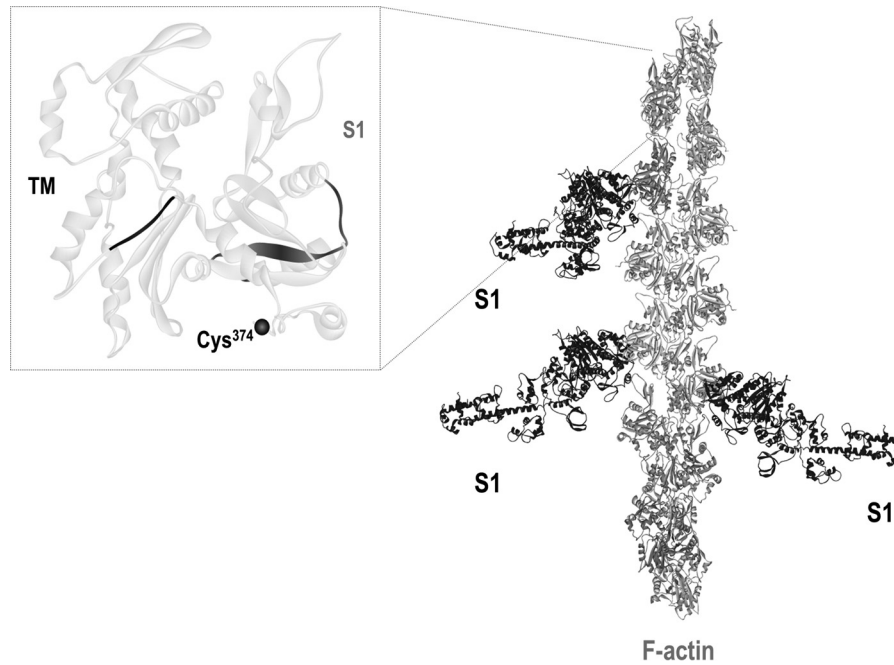
FIGURE 1. **Schematic representation of the interactions of actin, myosin, and tropomyosin.** *Left panel*, the structure of an actin monomer with the accurate position of Cys[374] (represented by a *black circle*), the site to which the fluorescent labels (IAEDANS or IAF) were attached. The TM (65) and S1 (66) binding sites in actin are highlighted in *black* and *gray*, respectively. *Right panel*, the structural view of an actin filament (F-actin) with bound S1. The figure is based on Protein Data Bank codes 2ZWH (for actin monomer) and 1MVW (for S1-decorated actin filament). The figure was made using WebLab ViewerPro 3.7 software.
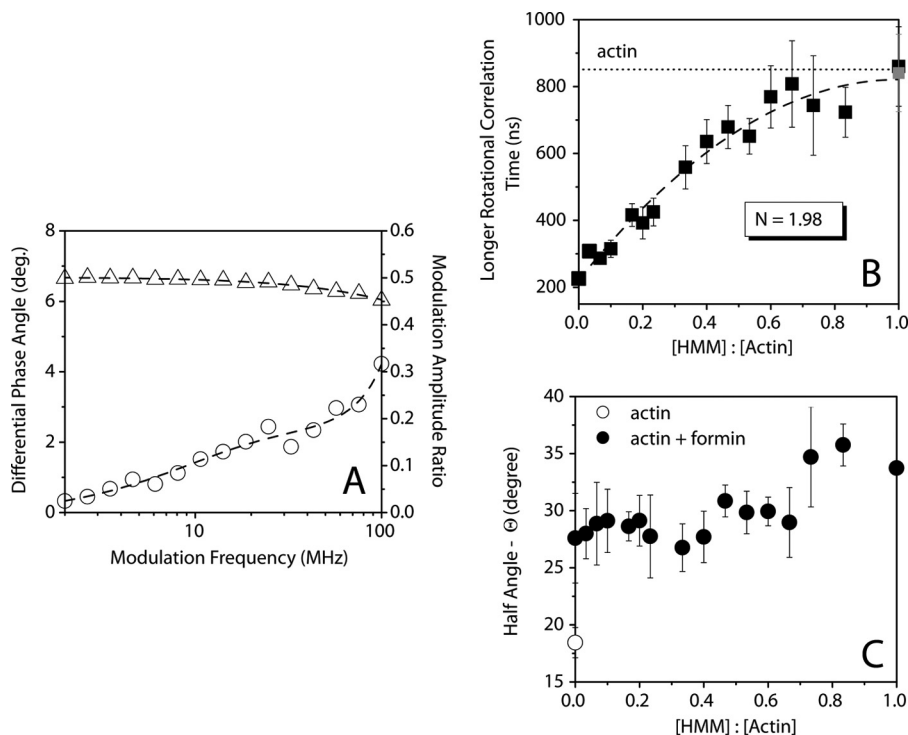

FIGURE 2. **HMM affects the anisotropy decay of formin-nucleated IAEDANS-actin filaments.** *A*, representative frequency-dependent phase (*empty circles*) and amplitude (*empty triangles*) data on a logarithmic plot and a corresponding fit (*dashed line*) with a double exponential function (Equation 5) from anisotropy decay measurements. *B*, the longer rotational correlation time measured as a function of the HMM:actin concentration ratio. The *dotted line* indicates the rotational correlation time characteristic for actin filaments in the absence of actin-binding proteins. The rotational correlation time of actin filaments measured in the absence of mDia1-FH2 and in presence of HMM is indicated by a *gray square*. Fitting the linear lattice model (Equation 7; shown as *dashed line*) gives $N = 1.98 \pm 0.2$ actin protomers for the length of the cooperative unit. *C*, the HMM:actin concentration ratio dependence of the half-angle of the cone (Θ) within which IAEDANS at Cys[374] performs wobbling motion in formin-nucleated actin filaments (*black circles*). The half-angle calculated for actin filaments in the absence of actin-binding proteins is represented by an *empty circle*. The actin and mDia1-FH2 concentrations were 30 and 1.25 μM, respectively. The *error bars* presented are standard errors from at least three independent experiments. *deg.*, degree.
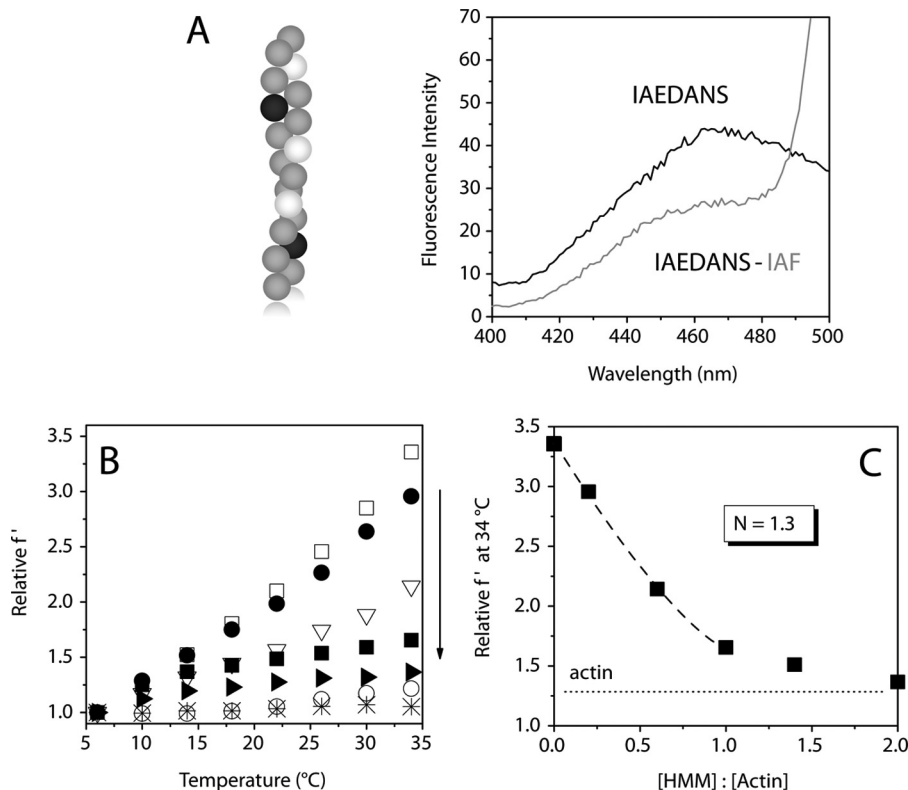
FIGURE 3. **HMM decreases the conformational flexibility of formin-nucleated actin filaments.** *A*, *left panel*, schematic representation of the position of the donors (*dark gray circles*) and acceptors (*light gray circles*) within the actin filament. *Empty circles* represent unlabeled actin protomers. This arrangement allows the characterization of the interprotomer conformational dynamics of the actin filaments. *Right panel*, representative fluorescence emission spectra of the donor measured in the absence (IAEDANS; *black line*) or presence (IAEDANS-IAF; *gray line*) of the acceptor in the absence of actin-binding proteins. *B*, temperature dependence of the relative f'. The experiments were carried out with 5 μM actin in the absence of actin-binding proteins (*empty circles*), in the presence of 500 nM mDia1-FH2 (*empty squares*), and in the presence of 500 nM mDia1-FH2 and 1 (*filled circles*), 3 (*empty triangles*), 5 (*filled squares*), or 10 μM (*filled triangles*) HMM. The *arrow* at the *right* indicates the increase of the HMM concentration and the decrease of actin filament flexibility. As a control, the temperature dependence of the relative f' characteristic for the actin-myosin complex is represented by *asterisks* (our previous unpublished data) showing that myosin binding does not significantly affect the temperature dependence of the relative f'. *C*, the relative f' at 34 °C as a function of the HMM:actin concentration ratio. The *dotted line* indicates the relative f' characteristic for actin filaments in the absence of actin-binding proteins. HMM concentrations are indicated as HMM head concentrations. Fitting the linear lattice model (Equation 7; shown as *dashed line*) gives $N = 1.30 \pm 0.1$ actin protomers for the length of the cooperative unit. The experiments were carried out with 5 μM actin, 500 nM mDia1-FH2, and HMM as indicated.

binding proteins, the longer rotational correlation time characteristic for actin filaments (30 μM) was ~800–900 ns (Fig. 2*B*, *dotted line*). Addition of HMM (30 μM) at the highest concentration did not change this value (Fig. 2*B*, *gray square*). In good agreement with our previous findings (21, 24), the rotational correlation time decreased to ~225 ns in the presence of mDia1-FH2 (1.25 μM) (Fig. 2*B*), showing that the binding of mDia1-FH2 results in a more flexible conformational state of the actin filaments. The anisotropy decay experiments with formin-nucleated actin filaments were repeated at different HMM concentrations (Fig. 2*B*). The longer rotational correlation time increased with increasing concentrations of HMM from 225 to ~850 ns (Fig. 2*B*). The increase indicates that the conformation of the formin-nucleated actin filaments is stiffer in the HMM-bound state. At higher HMM concentrations, the conformation of the actin filaments becomes similar to that observed in the absence of mDia1-FH2 and HMM.

To obtain further information regarding the HMM-induced conformational transitions and describe the microenvironment of IAEDANS at Cys[374], the two-dimensional angular range within which the fluorophore performs wobbling motion (half-angle, Θ) was calculated from the amplitudes of the two rotational modes using Equation 6 (44). The half-angle was

plotted as a function of the HMM:actin concentration ratio (Fig. 2*C*). In good agreement with our previous results (21), the value of Θ increased upon addition of mDia1-FH2 to actin filaments from 18.43 to 27.59°, indicating the increased freedom of the wobbling motion of IAEDANS in the formin-nucleated actin filaments. The half-angle did not change when HMM was added to the formin-nucleated actin filaments, suggesting that the microenvironment of the fluorescent probe was not affected by HMM. Thus, presumably the HMM-induced conformational stabilization of the formin-nucleated actin filaments originates from more global structural changes that do not affect the microenvironment of Cys[374].

As an alternative method, temperature-dependent FRET measurements were also performed to study the effects of HMM on the conformational dynamics of the formin-nucleated actin filaments (Fig. 3). The temperature dependence of the normalized f' (Equation 1) was measured between 6 and 34 °C using donor (IAEDANS) and acceptor (IAF) probes attached to the Cys[374] on actin (Fig. 1, *left panel*). The relative f' was calculated as the ratio of the value of f' at the given temperature and value of f' at the lowest temperature and plotted as a function of temperature (Fig. 3*B*). As a result of the applied preparation technique, one actin protomer bound only one

fluorophore (either a donor or an acceptor), and the FRET occurred between probes on neighboring protomers (Fig. 3*A*, *left panel*). This experimental strategy allowed the characterization of interprotomer conformational dynamics of actin filaments (6). In the evaluation of these experiments, the steeper temperature dependence of the relative *f*′ indicates a more flexible protein matrix between the donor and the acceptor (41, 42). The relative *f*′ of actin filaments (5 μM) in the absence of actin-binding proteins showed a ~25% increase over the investigated temperature range (Fig. 3*B*, *empty circles*). The presence of myosin did not significantly change this tendency (Fig. 3*B*, *asterisks*). In the presence of mDia1-FH2 (500 nM), the temperature profile of the relative *f*′ became steeper (increased by ~235%), indicating that the binding of mDia1-FH2 makes the actin filaments more flexible (Fig. 3*B*, *empty squares*). These formin-induced changes are in agreement with our previous observations (20). To describe the effect of myosin, HMM was added to the formin-nucleated actin filaments at different concentrations. The results showed that HMM decreased the effect of mDia1-FH2 in a concentration-dependent manner. When the concentration of HMM heads was the same as the actin concentration (*i.e.* 5 μM), the change in the relative *f*′ was 65%, whereas at a 2-fold higher HMM concentration relative to actin (*i.e.* 10 μM), the relative *f*′ changed by 36%. Fig. 3*C* summarizes the HMM concentration dependence of the FRET data assuming that the change in the relative *f*′ at the highest temperature (34 °C) is proportional to the conformational flexibility of actin filaments. In conclusion, corroborating the observations from the time-dependent anisotropy measurements, the FRET data indicate that the formin-induced increase in the flexibility of actin filaments is restored by the binding of HMM.

Cooperative Stabilization by HMM—To analyze the stabilizing effect of HMM in detail, we used the linear lattice model to estimate the number of actin protomers whose conformation is affected by the binding of a single HMM head (28). Equation 7 was fitted to the data presented in Figs. 2*B* and 3*C*. From anisotropy decay measurements, the length of the cooperative unit (*N*) was found to be 1.98 ± 0.2 actin protomers (Fig. 2*B*), indicating that the binding of one HMM head can stabilize the conformation of two actin protomers. The cooperative unit determined from temperature-dependent FRET measurements was found to be 1.30 ± 0.1 (Fig. 3*C*), which is somewhat smaller than that we obtained from the anisotropy decay experiments (1.98 ± 0.2; Fig. 2*B*). This difference indicates that the two methods are sensitive to different conformational transitions and modes of motions in the actin filaments. In conclusion, these results suggest that HMM stabilizes the structure of the formin-nucleated actin filaments cooperatively by affecting different conformational modes in the actin filament.

Kinetic Analysis of the Stabilizing Effects of HMM and TM—Our previous studies revealed that the formin-induced conformational transition could be reversed by the binding of TM to actin filaments (24). Here, we identified HMM as another binding partner of actin that stabilizes the structure of the formin-nucleated more flexible actin filaments. To get further insight into the stabilizing effects of HMM and TM, the kinetics of the conformational change induced by these proteins was investigated by monitoring the change in the steady-state anisotropy.

Steady-state anisotropy provides information about the conformational dynamics of the actin filaments: when appropriate conditions are fulfilled, the higher anisotropy value reflects the more restricted conformational dynamics of the protein matrix. We found that the steady-state anisotropy of IAE-DANS-actin is also sensitive to the formin-induced conformational changes (Fig. 4*A*). The steady-state anisotropy of actin filaments (5 μM) was 0.25–0.26 in the absence of actin-binding proteins (Fig. 4*A*, *light gray* curve). When actin was polymerized in the presence of mDia1-FH2 (500 nM), a slow, gradual decrease was observed in the steady-state anisotropy from the value characteristic for actin filaments to 0.14–0.17 (Fig. 4*A*, *black* curve). Essentially the same result was obtained when mDia1-FH2 was added to actin after the completion of polymerization (Fig. 4*A*, *dark gray* curve).

To study the effect of HMM and TM, these proteins were added to the formin-nucleated actin filaments after polymerization. In the presence of HMM, the steady-state anisotropy increased following an apparently exponential transient and reached a level that was typical for actin filaments alone (0.24–0.26) within ~1–5 min (Fig. 4*B*). Addition of TM to the formin-nucleated actin filaments also resulted in an increase in the steady-state anisotropy; however, a slightly lower plateau was reached at a longer timescale (~35 min) (Fig. 4*C*).

Steady-state anisotropy can also increase upon complex formation, *i.e.* upon only the binding of HMM or TM to actin filaments without any accompanying conformational changes. Control experiments were carried out to investigate how steady-state anisotropy of actin filaments (5 μM) changes upon the binding of HMM (20 μM) or TM (15 μM) to actin filaments. The results showed that the addition of HMM or TM to actin filaments caused only a minor increase in the steady-state anisotropy (~0.033 and ~0.001, respectively) (data not shown). HMM and TM bind actin and formin-nucleated actin filaments similarly (supplemental Fig. 4 and Ref. 24). From these observations, we concluded that complex formation cannot account for the anisotropy increase caused by HMM or TM in formin-nucleated actin filaments. The increase in the steady-state anisotropy of formin-nucleated actin filaments in the presence of HMM or TM reflects mostly the conformational stabilization of actin filaments by HMM and TM.

The steady-state anisotropy data were analyzed by fitting single exponential functions to the observed transients (Equation 3). The amplitudes resolved in these fits gave the Δr induced by the binding of either HMM or TM and were plotted as a function of protein concentration in Fig. 5, *A* and *B*. A hyperbolic function was fit to the data (Equation 4) to obtain the values of the maximum change (Max) and half-saturation protein concentrations ($K_{\frac{1}{2}}$) (Fig. 5, *A* and *B*). For HMM, the maximum anisotropy increase was 0.198 ± 0.01, and the half-saturation was reached at 7.07 ± 1.3 μM HMM. This value is close to the applied actin concentration (5 μM). For TM, we observed a maximum amplitude of 0.103 ± 0.0. This value is somewhat smaller than that found with HMM, suggesting that HMM is more effective in stabilizing the structure of the formin-nucleated actin filaments than TM. The half-maximum was determined to be 0.33 ± 0.1 μM for TM. This half-saturation concentration is about 10-fold less than was observed for HMM,
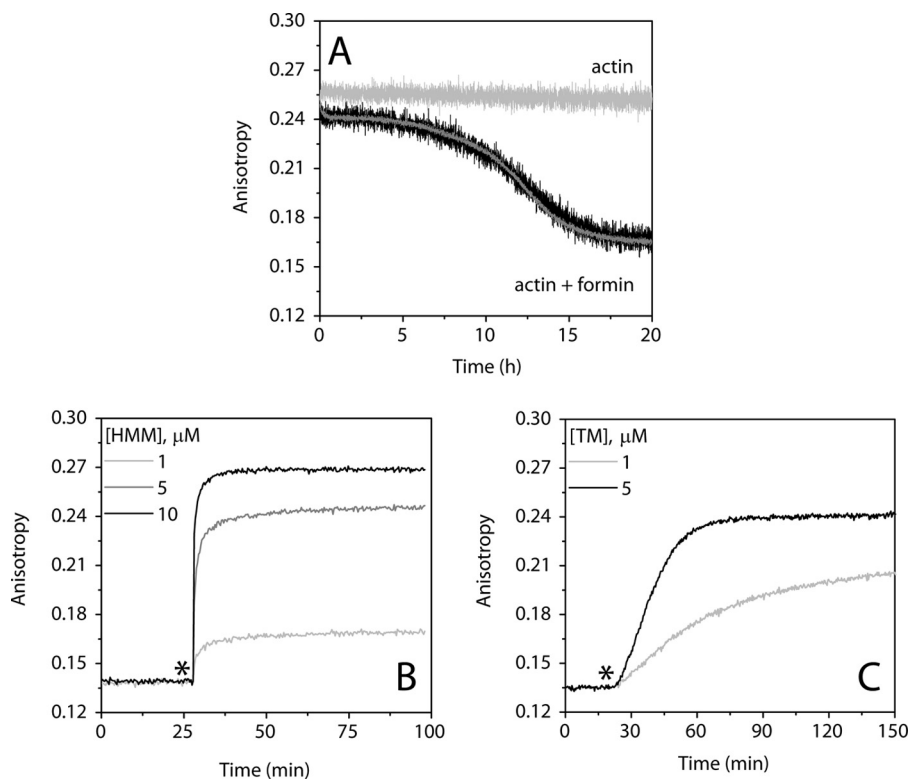
FIGURE 4. **The effect of HMM and TM on the conformational dynamics of formin-nucleated actin filaments revealed by steady-state anisotropy.** *A,* the kinetics of the change in the steady-state anisotropy of IAEDANS-actin filaments (5 μM) measured in the absence (*light gray* curve) or in the presence of 500 nM mDia1-FH2 (*black* curve). *Black* and *dark gray* curves show the results obtained when mDia1-FH2 was added to actin prior or after polymerization, respectively. Note that the curves are superimposable. *B,* the kinetics of the change in the steady-state anisotropy of mDia1-FH2-nucleated (500 nM) IAEDANS-actin filaments (5 μM) measured at different HMM concentrations as indicated Representative data are shown. Note that the steady-state anisotropy started to increase right after the addition of HMM (indicated by an *asterisk*) and plateaued within ~1–5 min. *C,* the kinetics of the change in the steady-state anisotropy of mDia1-FH2-nucleated (500 nM) IAEDANS-actin filaments (5 μM) measured in the presence of different TM concentrations as indicated. Representative data are shown. Note that the steady-state anisotropy started to increase right after the addition of TM (indicated by an *asterisk*) and plateaued within ~30 min.

corresponding to the fact that one TM interacts with seven actin monomers in a filament (51).

We also analyzed the HMM and TM concentration dependence of the rate constants (k_{obs}) derived from the exponential fits (Fig. 5, *C* and *D*). In the case of HMM, the k_{obs} values followed a quasilinear tendency with increasing amount of HMM (Fig. 5*C*). This kinetic behavior indicates that HMM binding to the formin-nucleated actin filaments occurs as an apparent single step reaction. Interestingly, the slope of the fit reflecting an apparent association rate constant of 0.004 μM^{-1} s^{-1} was much lower than that determined from stopped-flow measurements based on pyrene-actin fluorescence intensity changes upon HMM binding to actin filaments. The latter value was 22.6 μM^{-1} s^{-1}, which is independent from the presence of mDia1-FH2 (supplemental Fig. 4). This value is close to the value obtained for skeletal muscle S1 (10 μM^{-1} s^{-1} (52–54)). However, it should be emphasized that the large difference from the present result may at least in part originate from the fact that different types of signal can indicate different structural changes during the actin binding process. For TM, the k_{obs} *versus* TM concentration curve showed a saturating tendency (Fig. 5*D*). This kinetic behavior is indicative of a two-step reaction in which the added TM binds to the actin filament, and then a first-order conformational transition occurs in the complex. Interestingly, the maximal observed rate constant, reflecting the first-order transition, was much lower than the rate con-

stants observed in the case of HMM (Fig. 5*C*). These findings imply that, despite the apparently similar reversal of formin-induced conformational changes by HMM and TM, the kinetic mechanism of this process is markedly different in the case of these two actin-binding proteins.

We performed control experiments (supplemental Experimental Procedures) to study whether the different experimental conditions (temperature, fluorescent labels, and the presence of the investigated proteins) affect the actin monomer: filament ratio, the length distribution of actin filament, and the activity of mDia1-FH2. The experiments and the results are summarized and discussed in the supplemental material. From the results of these control experiments, we concluded that none of the experimental conditions significantly change the actin monomer:filament ratio (supplemental Fig. 1), the length distribution of actin filament (supplemental Fig. 2 and Table 1), and the activity of mDia1-FH2 (supplemental Fig. 3).

DISCUSSION

Our previous spectroscopic studies revealed that the binding of formin to the barbed end of actin filaments changes the conformation of several actin protomers, making the filaments more flexible (20–22). The biological significance of the formin-induced conformational transitions in actin filaments is still unclear. Most of the functions attributed to actin networks require a certain and probably optimized mechanical stability
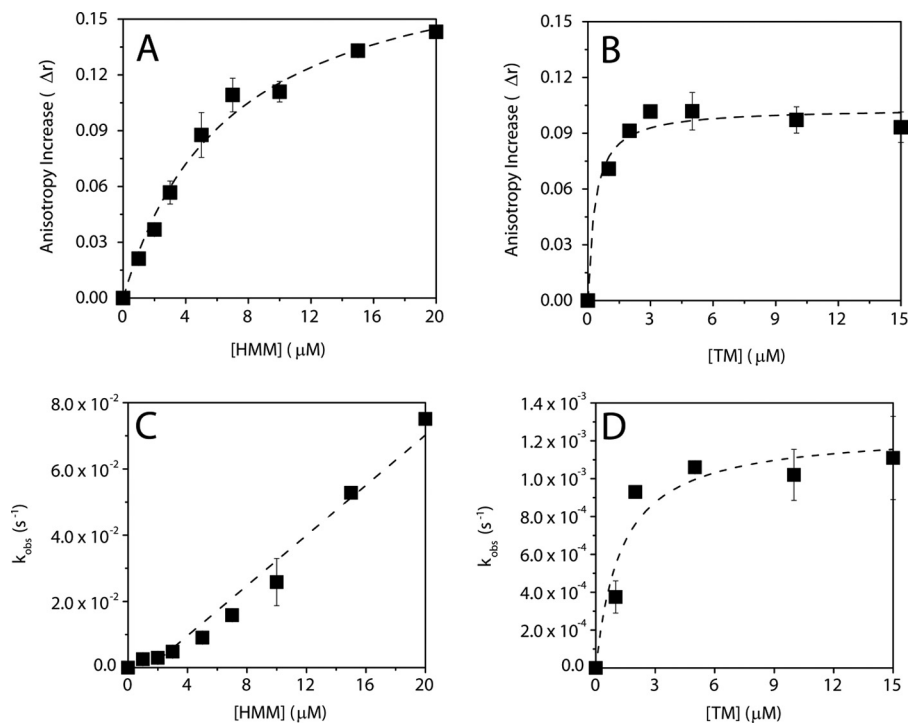
FIGURE 5. **The analysis of the effects of HMM and TM on the formin-induced conformational changes in actin filaments.** *A* and *B*, Δr as a function of HMM (*A*) or TM (*B*) concentration. The anisotropy increase was derived from the exponential fit (Equation 3) of the data presented in Fig. 4, *B* and *C*. Note that a higher increase in the steady-state anisotropy from the low value of ~0.14 (characteristic for mDia1-FH2-nucleated actin filaments) indicates a greater stabilization of the conformational dynamics of mDia1-FH2-nucleated actin filaments. The data were analyzed by hyperbolic fits (Equation 4) (*dashed lines*). The maximum values (Max) were 0.198 ± 0.01 and 0.103 ± 0.00 for HMM and TM, respectively. The half-saturation concentrations ($K_{1/2}$) were determined to be 7.07 ± 1.3 and 0.33 ± 0.1 μM for HMM and TM, respectively. *C* and *D*, the observed rate constants (k_{obs}) as a function of HMM (*C*) or TM (*D*) concentration. The values of k_{obs} were derived from the exponential fit (Equation 3) of the data presented in Fig. 4, *B* and *C*. The stabilizing effect of HMM on mDia1-FH2-nucleated actin filaments was rapid, and the observed rate constant increased linearly with increasing amount of HMM. The apparent on-rate constant of anisotropy change determined from the slope of the linear fit was 0.004 μM^{-1} s^{-1}. The stabilizing effect of TM on mDia1-FH2-nucleated actin filaments was much slower than that of HMM and followed a hyperbolic tendency with increasing TM concentration. The *error bars* presented on this figure are standard errors from at least two independent experiments.

and rigidity of the filaments (55–57). It is therefore reasonable to expect that actin-binding proteins could reverse the formin-induced structural changes by binding to filaments. Obvious candidates for this stabilizing function could be those proteins that often co-localize with formin-generated actin structures in cells. One of these proteins, TM, was recently shown to stabilize the conformation of formin-nucleated actin filaments (24). We assumed that another candidate for the stabilization function could be myosin, an abundant binding partner of formin-generated actin networks (25, 58, 59). The data presented in this work show that HMM restores the formin-induced conformational changes in the actin filaments and stabilizes the structure of the filaments, resulting in actin filament conformation similar to that observed in the absence of formin and myosin.

The detailed analysis of time-dependent anisotropy data suggests that the microenvironment of the fluorophore was not affected by HMM (Fig. 2*C*), indicating that the HMM-induced conformational stabilization of the formin-nucleated actin filaments originates from more global structural changes. The length of the cooperative unit was estimated to be 1.98 ± 0.2 actin protomers (Fig. 2*B*) from anisotropy decay experiments, suggesting that the binding of one HMM head stabilizes the structure of two actin protomers. Similar long range allosteric interactions, often called cooperativity in actin filaments, were reported for actin filaments in many cases previously (8, 9, 27, 60–62). Recent transient phosphorescence anisotropy experi-

ments revealed that in the strong binding state skeletal muscle S1 restricted the conformational dynamics of actin filaments in a cooperative manner (31). The experimental conditions in this cited work differed from our measurements in a few important aspects: the experiments were carried out with phalloidin-stabilized actin filaments, the myosin fragments were single-headed, and formin was not involved in the measurements. Most importantly, because of the difference in the lifetime of the fluorophores and thus the time window of observation, phosphorescence experiments allow the accurate measurements of rotational correlation times of a few hundreds of microseconds, which are unresolvable by our fluorescence approach. The microsecond rotational correlation times can characterize different conformational modes within actin filaments related to the twisting and bending of actin filaments (10, 63). Interestingly, despite these substantial differences in experimental approaches, the conclusions regarding the cooperativity of the conformational changes induced by the skeletal muscle myosin fragments were similar in the two studies. Analysis of the S1 concentration dependence of the rotational correlation times obtained from phosphorescence anisotropy measurements gave 1.9 ± 0.5 actin protomers for the length of the cooperative unit (31), which is the same as we found here for HMM (1.98 ± 0.2) based on fluorescence anisotropy experiments. This observation suggests that myosin can similarly stabilize these different conformational modes of actin filaments.

In temperature-dependent FRET measurements, the saturating effect of HMM was close to a 1:1 HMM:actin concentration ratio (Fig. 3), and the length of the cooperative unit was found to be shorter (1.30 ± 0.1) than in the anisotropy decay experiments. This difference may be explained considering that the two methods are sensitive to different aspects of actin filament conformation and flexibility. The longer rotational correlation time provides information on a time scale of a few hundreds of nanoseconds, and it is sensitive to the changes in the restricted segmental motion of one or more protomers in the actin filaments. The relative f' reflects changes in all kinds of intramolecular motions within actin filaments from smaller local fluctuations to large scale filament motions, which alter the relative position of the donor and acceptor (50). Thus, the difference between the length of the cooperative unit (1.98 ± 0.2 *versus* 1.30 ± 0.1 protomers) obtained by the two methods indicates that the conformational transitions in actin are complex, and the binding of HMM can affect the various modes of the intramolecular actin motions differently. Similar uncoupling of the molecular events defining the values of various spectroscopic parameters was found previously in actin filaments (31).

Both the anisotropy decay and FRET data presented here showed that HMM can reverse the formin-induced conformational changes in actin. Considering the observation that TM also stabilizes the structure of the actin filaments, one can assume that actin-binding proteins play a central role in the molecular mechanisms regulating the conformational dynamics of actin filaments. We speculate that the greater flexibility of the filaments observed in the presence of formins may result from the rapid and unique manner of formin-catalyzed polymerization. For certain functions of actin filaments, like force-generating actin filaments in stress fibers or the contractile ring, the conformational state with a more rigid structure is likely preferable. Thus, molecular mechanisms exist that reverse the formin-induced flexibility changes. These mechanisms are based on the binding of actin-associated proteins to actin filaments. In cellular structures, formins provide the rapid assembly of actin filaments, and then the subsequent binding of regulatory proteins establishes the appropriate conformational features for a given cellular task. With the results presented here, there are now two abundant binding partners of actin identified, TM and HMM, that can play such regulatory roles. Their common property is that the binding of both of these proteins cooperatively affects the structure of the actin filaments along a stretch of several protomers. In our *in vitro* measurements with purified proteins, the HMM- and TM-induced conformational stabilization of actin filaments occurs on the minute time scale. Considering the kinetics of the *in vivo* processes, we expect that there are cellular factors that can accelerate the rate of the stabilizing mechanism (64).

Further investigations are needed to identify other actin-binding proteins that play a regulatory role in the fine tuning of actin conformation. These proteins should be studied in complex systems to reveal how the different effects of actin-binding proteins on the conformational properties of actin are superimposed (synergistically or antagonistically) to establish the overall conformational dynamics and biological function of cellular actin structures.

REFERENCES

1. Pollard, T. D., and Cooper, J. A. (2009) Actin, a central player in cell shape and movement. *Science* **326,** 1208–1212
2. Le Clainche, C., and Carlier, M. F. (2008) Regulation of actin assembly associated with protrusion and adhesion in cell migration. *Physiol. Rev.* **88,** 489–513
3. Chhabra, E. S., and Higgs, H. N. (2007) The many faces of actin: matching assembly factors with cellular structures. *Nat. Cell Biol.* **9,** 1110–1121
4. Miki, M., Wahl, P., and Auchet, J. C. (1982) Fluorescence anisotropy of labeled F-actin: influence of divalent cations on the interaction between F-actin and myosin heads. *Biochemistry* **21,** 3661–3665
5. Hild, G., Nyitrai, M., and Somogyi, B. (2002) Intermonomer flexibility of Ca- and Mg-actin filaments at different pH values. *Eur. J. Biochem.* **269,** 842–849
6. Nyitrai, M., Hild, G., Hartvig, N., Belágyi, J., and Somogyi, B. (2000) Conformational and dynamic differences between actin filaments polymerized from ATP- or ADP-actin monomers. *J. Biol. Chem.* **275,** 41143–41149
7. Nyitrai, M., Hild, G., Belágyi, J., and Somogyi, B. (1999) The flexibility of actin filaments as revealed by fluorescence resonance energy transfer. The influence of divalent cations. *J. Biol. Chem.* **274,** 12996–13001
8. Visegrády, B., Lorinczy, D., Hild, G., Somogyi, B., and Nyitrai, M. (2004) The effect of phalloidin and jasplakinolide on the flexibility and thermal stability of actin filaments. *FEBS Lett.* **565,** 163–166
9. Prochniewicz, E., Zhang, Q., Janmey, P. A., and Thomas, D. D. (1996) Cooperativity in F-actin: binding of gelsolin at the barbed end affects structure and dynamics of the whole filament. *J. Mol. Biol.* **260,** 756–766
10. Prochniewicz, E., Henderson, D., Ervasti, J. M., and Thomas, D. D. (2009) Dystrophin and utrophin have distinct effects on the structural dynamics of actin. *Proc. Natl. Acad. Sci. U.S.A.* **106,** 7822–7827
11. Galkin, V. E., Orlova, A., VanLoock, M. S., Shvetsov, A., Reisler, E., and Egelman, E. H. (2003) ADF/cofilin use an intrinsic mode of F-actin instability to disrupt actin filaments. *J. Cell Biol.* **163,** 1057–1066
12. Prochniewicz, E., Janson, N., Thomas, D. D., and De la Cruz, E. M. (2005) Cofilin increases the torsional flexibility and dynamics of actin filaments. *J. Mol. Biol.* **353,** 990–1000
13. Kudryashov, D. S., Galkin, V. E., Orlova, A., Phan, M., Egelman, E. H., and Reisler, E. (2006) Cofilin cross-bridges adjacent actin protomers and replaces part of the longitudinal F-actin interface. *J. Mol. Biol.* **358,** 785–797
14. Sellers, J. R. (ed) (1999) *Protein Profile: Myosins*, 2nd Ed., Oxford University Press, Oxford
15. Pollard, T. D. (2007) Regulation of actin filament assembly by Arp2/3 complex and formins. *Annu. Rev. Biophys. Biomol. Struct.* **36,** 451–477
16. Renault, L., Bugyi, B., and Carlier, M. F. (2008) Spire and Cordon-bleu: multifunctional regulators of actin dynamics. *Trends Cell Biol.* **18,** 494–504
17. Bugyi, B., and Carlier, M. F. (2010) Control of actin filament treadmilling in cell motility. *Annu. Rev. Biophys.* **39,** 449–470
18. Chesarone, M. A., DuPage, A. G., and Goode, B. L. (2010) Unleashing formins to remodel the actin and microtubule cytoskeletons. *Nat. Rev. Mol. Cell Biol.* **11,** 62–74
19. Wen, K. K., and Rubenstein, P. A. (2009) Differential regulation of actin polymerization and structure by yeast formin isoforms. *J. Biol. Chem.* **284,** 16776–16783
20. Bugyi, B., Papp, G., Hild, G., Lõrinczy, D., Nevalainen, E. M., Lappalainen, P., Somogyi, B., and Nyitrai, M. (2006) Formins regulate actin filament flexibility through long range allosteric interactions. *J. Biol. Chem.* **281,** 10727–10736
21. Papp, G., Bugyi, B., Ujfalusi, Z., Barkó, S., Hild, G., Somogyi, B., and Nyitrai, M. (2006) Conformational changes in actin filaments induced by formin binding to the barbed end. *Biophys. J.* **91,** 2564–2572
22. Ujfalusi, Z., Barkó, S., Hild, G., and Nyitrai, M. (2010) The effects of formins on the conformation of subdomain 1 in actin filaments. *J. Photochem. Photobiol. B* **98,** 7–11

23. Kupi, T., Gróf, P., Nyitrai, M., and Belagyi, J. (2009) The uncoupling of the effects of formins on the local and global dynamics of actin filaments. *Biophys. J.* **96,** 2901–2911

24. Ujfalusi, Z., Vig, A., Hild, G., and Nyitrai, M. (2009) Effect of tropomyosin on formin-bound actin filaments. *Biophys. J.* **96,** 162–168

25. Tojkander, S., Gateva, G., Schevzov, G., Hotulainen, P., Naumanen, P., Martin, C., Gunning, P. W., and Lappalainen, P. (2011) A molecular pathway for myosin II recruitment to stress fibers. *Curr. Biol.* **21,** 539–550

26. Kovar, D. R., Sirotkin, V., and Lord, M. (2011) Three's company: the fission yeast actin cytoskeleton. *Trends Cell Biol.* **21,** 177–187

27. Orlova, A., and Egelman, E. H. (1997) Cooperative rigor binding of myosin to actin is a function of F-actin structure. *J. Mol. Biol.* **265,** 469–474

28. Prochniewicz, E., and Thomas, D. D. (1997) Perturbations of functional interactions with myosin induce long-range allosteric and cooperative structural changes in actin. *Biochemistry* **36,** 12845–12853

29. Prochniewicz, E., and Thomas, D. D. (2001) Site-specific mutations in the myosin binding sites of actin affect structural transitions that control myosin binding. *Biochemistry* **40,** 13933–13940

30. Prochniewicz, E., Walseth, T. F., and Thomas, D. D. (2004) Structural dynamics of actin during active interaction with myosin: different effects of weakly and strongly bound myosin heads. *Biochemistry* **43,** 10642–10652

31. Prochniewicz, E., Chin, H. F., Henn, A., Hannemann, D. E., Olivares, A. O., Thomas, D. D., and De La Cruz, E. M. (2010) Myosin isoform determines the conformational dynamics and cooperativity of actin filaments in the strongly bound actomyosin complex. *J. Mol. Biol.* **396,** 501–509

32. Feuer, G., Molnár, F., Pettkó, E., and Straub, F. B. (1948) Studies on the composition and polymerization of actin. *Hung. Acta Physiol.* **1,** 150–163

33. Spudich, J. A., and Watt, S. (1971) The regulation of rabbit skeletal muscle contraction. I. Biochemical studies of the interaction of the tropomyosin-troponin complex with actin and the proteolytic fragments of myosin. *J. Biol. Chem.* **246,** 4866–4871

34. Houk, T. W., Jr., and Ue, K. (1974) The measurement of actin concentration in solution: a comparison of methods. *Anal. Biochem.* **62,** 66–74

35. Elzinga, M., Collins, J. H., Kuehl, W. M., and Adelstein, R. S. (1973) Complete amino-acid sequence of actin of rabbit skeletal muscle. *Proc. Natl. Acad. Sci. U.S.A.* **70,** 2687–2691

36. Shimada, A., Nyitrai, M., Vetter, I. R., Kühlmann, D., Bugyi, B., Narumiya, S., Geeves, M. A., and Wittinghofer, A. (2004) The core FH2 domain of diaphanous-related formins is an elongated actin binding protein that inhibits polymerization. *Mol. Cell* **13,** 511–522

37. Margossian, S. S., and Lowey, S. (1982) Preparation of myosin and its subfragments from rabbit skeletal muscle. *Methods Enzymol.* **85,** 55–71

38. Smillie, L. B. (1982) Preparation and identification of α- and β-tropomyosins. *Methods Enzymol.* **85,** 234–241

39. Miki, M., dos Remedios, C. G., and Barden, J. A. (1987) Spatial relationship between the nucleotide-binding site, Lys-61 and Cys-374 in actin and a conformational change induced by myosin subfragment-1 binding. *Eur. J. Biochem.* **168,** 339–345

40. Hudson, E. N., and Weber, G. (1973) Synthesis and characterization of two fluorescent sulfhydryl reagents. *Biochemistry* **12,** 4154–4161

41. Somogyi, B., Lakos, Z., Szarka, A., and Nyitrai, M. (2000) Protein flexibility as revealed by fluorescence resonance energy transfer: an extension of the method for systems with multiple labels. *J. Photochem. Photobiol. B* **59,** 26–32

42. Somogyi, B., Matkó, J., Papp, S., Hevessy, J., Welch, G. R., and Damjanovich, S. (1984) Förster-type energy transfer as a probe for changes in local fluctuations of the protein matrix. *Biochemistry* **23,** 3403–3411

43. Lakowicz, J. R. (2006) *Principles of Fluorescence Spectroscopy*, 3rd ed., pp. 161–163, Springer, New York

44. Kinosita, K., Jr., Kawato, S., and Ikegami, A. (1977) A theory of fluorescence polarization decay in membranes. *Biophys. J.* **20,** 289–305

45. Romero, S., Didry, D., Larquet, E., Boisset, N., Pantaloni, D., and Carlier, M. F. (2007) How ATP hydrolysis controls filament assembly from profilin-actin: implication for formin processivity. *J. Biol. Chem.* **282,** 8435–8445

46. Romero, S., Le Clainche, C., Didry, D., Egile, C., Pantaloni, D., and Carlier, M. F. (2004) Formin is a processive motor that requires profilin to accelerate actin assembly and associated ATP hydrolysis. *Cell* **119,** 419–429

47. Kovács, M., Thirumurugan, K., Knight, P. J., and Sellers, J. R. (2007) Load-dependent mechanism of nonmuscle myosin 2. *Proc. Natl. Acad. Sci. U.S.A.* **104,** 9994–9999

48. Hild, G., Nyitrai, M., Belágyi, J., and Somogyi, B. (1998) The influence of divalent cations on the dynamic properties of actin filaments: a spectroscopic study. *Biophys. J.* **75,** 3015–3022

49. Nyitrai, M., Hild, G., Belágyi, J., and Somogyi, B. (1997) Spectroscopic study of conformational changes in subdomain 1 of G-actin: influence of divalent cations. *Biophys. J.* **73,** 2023–2032

50. Hild, G., Bugyi, B., and Nyitrai, M. (2010) Conformational dynamics of actin: effectors and implications for biological function. *Cytoskeleton* **67,** 609–629

51. Yang, Y. Z., Korn, E. D., and Eisenberg, E. (1979) Cooperative binding of tropomyosin to muscle and *Acanthamoeba* actin. *J. Biol. Chem.* **254,** 7137–7140

52. Taylor, E. W. (1991) Kinetic studies on the association and dissociation of myosin subfragment 1 and actin. *J. Biol. Chem.* **266,** 294–302

53. Coates, J. H., Criddle, A. H., and Geeves, M. A. (1985) Pressure-relaxation studies of pyrene-labelled actin and myosin subfragment 1 from rabbit skeletal muscle. Evidence for two states of acto-subfragment 1. *Biochem. J.* **232,** 351–356

54. Takács, B., O'Neall-Hennessey, E., Hetényi, C., Kardos, J., Szent-Györgyi, A. G., and Kovács, M. (2011) Myosin cleft closure determines the energetics of the actomyosin interaction. *FASEB J.* **25,** 111–121

55. Kueh, H. Y., and Mitchison, T. J. (2009) Structural plasticity in actin and tubulin polymer dynamics. *Science* **325,** 960–963

56. Elson, E. L. (1988) Cellular mechanics as an indicator of cytoskeletal structure and function. *Annu. Rev. Biophys. Biophys. Chem.* **17,** 397–430

57. Condeelis, J. (1993) Life at the leading edge: the formation of cell protrusions. *Annu. Rev. Cell Biol.* **9,** 411–444

58. Yu, J. H., Crevenna, A. H., Bettenbühl, M., Freisinger, T., and Wedlich-Söldner, R. (2011) Cortical actin dynamics driven by formins and myosin V. *J. Cell Sci.* **124,** 1533–1541

59. Zigmond, S. H., Evangelista, M., Boone, C., Yang, C., Dar, A. C., Sicheri, F., Forkey, J., and Pring, M. (2003) Formin leaky cap allows elongation in the presence of tight capping proteins. *Curr. Biol.* **13,** 1820–1823

60. Orlova, A., Prochniewicz, E., and Egelman, E. H. (1995) Structural dynamics of F-actin: II. cooperativity in structural transitions. *J. Mol. Biol.* **245,** 598–607

61. Steinmetz, M. O., Goldie, K. N., and Aebi, U. (1997) A correlative analysis of actin filament assembly, structure, and dynamics. *J. Cell Biol.* **138,** 559–574

62. Visegrády, B., Lorinczy, D., Hild, G., Somogyi, B., and Nyitrai, M. (2005) A simple model for the cooperative stabilisation of actin filaments by phalloidin and jasplakinolide. *FEBS Lett.* **579,** 6–10

63. Prochniewicz, E., Zhang, Q., Howard, E. C., and Thomas, D. D. (1996) Microsecond rotational dynamics of actin: spectroscopic detection and theoretical simulation. *J. Mol. Biol.* **255,** 446–457

64. Berro, J., Sirotkin, V., and Pollard, T. D. (2010) Mathematical modeling of endocytic actin patch kinetics in fission yeast: disassembly requires release of actin filament fragments. *Mol. Biol. Cell* **21,** 2905–2915

65. Brown, J. H., Zhou, Z., Reshetnikova, L., Robinson, H., Yammani, R. D., Tobacman, L. S., and Cohen, C. (2005) Structure of the mid-region of tropomyosin: bending and binding sites for actin. *Proc. Natl. Acad. Sci. U.S.A.* **102,** 18878–18883

66. Labbé, J. P., Boyer, M., Roustan, C., and Benyamin, Y. (1992) Localization of a myosin subfragment-1 interaction site on the C-terminal part of actin. *Biochem. J.* **284,** 75–79